

# Network Complexity and Stability of Microbes Enhanced by Microplastic Diversity

Hao Wu,<sup>||</sup> Tianheng Gao,<sup>||</sup> Ang Hu, and Jianjun Wang\*



Cite This: *Environ. Sci. Technol.* 2024, 58, 4334–4345



Read Online

ACCESS |



Metrics & More



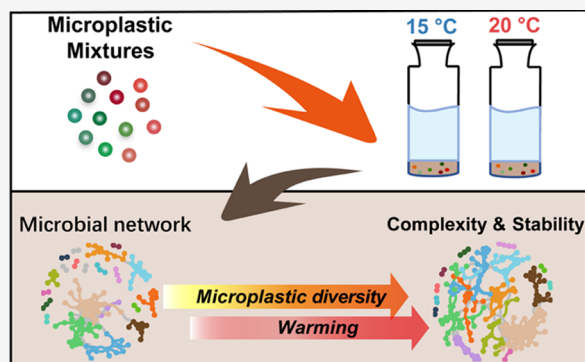
Article Recommendations



Supporting Information

**ABSTRACT:** Microplastic mixtures are ubiquitously distributed in global ecosystems and include varying types. However, it remains unknown how microplastic diversity affects the biotic interactions of microbes. Here, we developed novel experiments of 600 microcosms with microplastic diversity ranging from 1 to 6 types and examined ecological networks for microbial communities in lake sediments after 2 months of incubation at 15 and 20 °C. We found that microplastic diversity generally enhanced the complexity of microbial networks at both temperatures, such as increasing network connectance and reducing average path length. This phenomenon was further confirmed by strengthened species interactions toward high microplastic diversity except for the negative interactions at 15 °C. Interestingly, increasing temperatures further exaggerated the effects of microplastic diversity on network structures, resulting in higher network connectivity and species interactions. Consistently, using species extinction simulations, we found that higher microplastic diversity and temperature led to more robust networks, and their effects were additionally and positively mediated by the presence of biodegradable microplastics. Our findings provide the first evidence that increasing microplastic diversity could unexpectedly promote the complexity and stability of microbial networks and that future warming could amplify this effect.

**KEYWORDS:** *microplastic diversity, lake sediments, global warming, microbial network*



## INTRODUCTION

Microplastics are ubiquitously distributed in the Earth's ecosystems and are becoming increasingly diverse.<sup>1–3</sup> In global lakes and reservoirs, microplastic concentrations range from 0.001 to 10 particles m<sup>-3</sup> as revealed by a recent standardized large-scale survey.<sup>4</sup> Those small plastic debris with size less than 5 mm could comprise various types and cause serious ecological environmental problems such as posing multiple threats to micro- and macroorganisms.<sup>5–7</sup> These problems may be exaggerated by the interactive effects of microplastic mixtures, as different types of microplastics should be blended in the environments instead of existing separately.<sup>7</sup> For instance, rainwater samples collected in urban and peri-urban areas of Eastern India contained nine types of microplastics.<sup>8</sup> Thus, environmental microplastic mixtures also contain immense diversity such as the number of microplastic types.<sup>9</sup> However, to date, few experiments have considered the effects of microplastic mixtures and their diversity on biotic communities in ecosystems, which led to a lack of comprehensive understanding of microplastic pollution.

The effects of microplastics on microbial communities could be complex, such as influencing their structural hierarchy, biotic interaction, activity, and biodiversity.<sup>10–13</sup> On the one hand, various types of microplastics such as polypropylene

could release more bioavailable carbon sources during degradation than natural organic matters, which further stimulate the metabolism of microorganisms.<sup>14,15</sup> On the other hand, microplastics could function as unique and active substrates that attract surrounding microorganisms and further affect microbial species interactions.<sup>16,17</sup> More intriguingly, these effects may be further complicated by the mixing of various types of microplastics. For instance, microbial networks are more complex on the surface of polybutylene-adipate-terephthalate/poly lactide mixtures (PBAT/PLA) compared to single polyethylene (PE).<sup>18</sup> We expect that as the diversity of microplastics increased (e.g., types of microplastics), the complexity and stability of microbial networks could be further influenced, such as the enhanced network connectance and robustness (Figure 1a). We also expect that the biodegradability of microplastics could have potential impacts on shaping microbial networks.<sup>18,19</sup> Thus, predicting alterations in micro-

**Received:** October 19, 2023

**Revised:** December 16, 2023

**Accepted:** February 5, 2024

**Published:** February 21, 2024



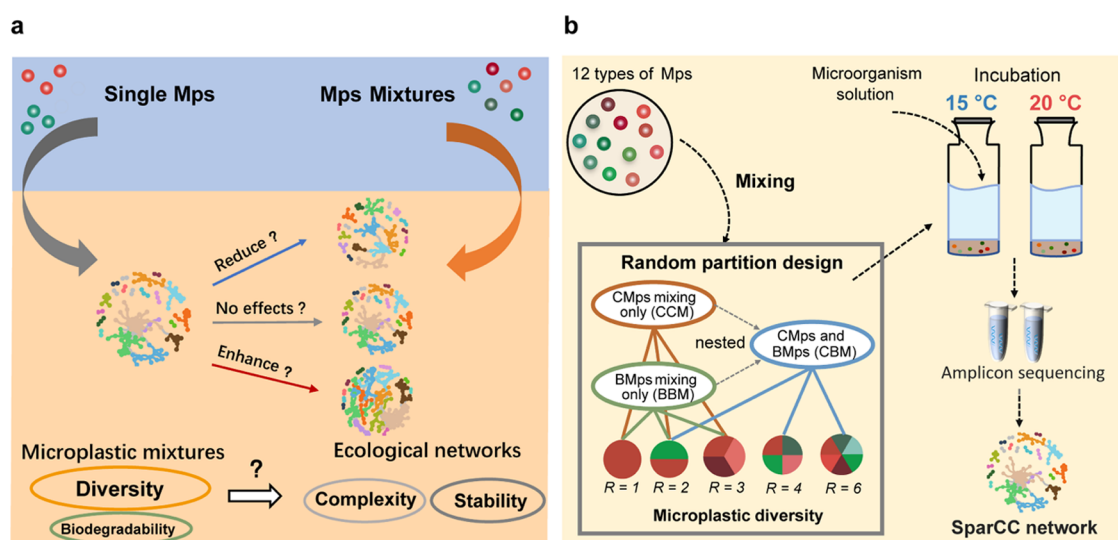


**Figure 1.** Study objectives and experimental design. (a) We expect that more types of environmental microplastics will enhance, weaken, or show nonsignificant effects on the complexity or stability of microbial networks (e.g., network connectance and modularity), which may be driven by the diversity (e.g., numbers of microplastic types) and biodegradability of microplastics. (b) Experimental layout. We selected 12 types of conventional and biodegradable microplastics (that is, CMPs and BMPs) and combined them to create the microplastic diversity gradients from 1 to 6 types using a random partition design.<sup>25</sup> We examined three possible microplastic mixing strategies presented in the natural environments, including mixing only CMPs and BMPs (CCM and BBM groups) and nesting the CMPs and BMPs with a consistent ratio of 1:1 (CBM group). We added each microcosm (sterilized 20 mL glass bottle) with 3 g of homogenized dried sediment, 0.12 g of microplastic mixtures, 1 mL of microbial suspension obtained from sediments of Taihu Lake, and 9 mL of sterile water. Each sample was performed with four replicates. Totally, we obtained 600 microcosms and incubated them at two temperatures of 15 and 20 °C. After 45 days of incubation, we determined the bacterial community structures in the microcosms and constructed the networks using the method of SparCC. Detailed information on experimental design is available in the [Materials and Methods](#) Section and [Table 1](#).

**Table 1.** Information about Microplastic Compositions of Experimental Design<sup>a</sup>

microplastic richness	groups (numbers)	compositions
1-microplastic	CCM (6) BBM (6)	PP/PE/PET/PS/PA/PVC PLA/PHA/PVA/PBAT/PBS/PCL
2-microplastics	CCM (9) BBM (9) CBM (18)	PP, PA/PE, PS/PET, PVC/PP, PS/PE, PET/PA, PVC/PP, PVC/PE, PA/PS, PET PLA, PCL/PBS, PBAT/PVA, PHA/PVA, PBAT/PLA, PHA/PBS, PCL/PLA, PBS/PHA, PBAT/PCL, PVA PP, PLA/PE, PCL/PA, PVA/PS, PBS/PET, PHA/PVC, PBAT/PP, PVA/PE, PBS/PA, PHA/PS, PCL/PET, PBAT/PVC, PLA/PP, PBAT/PE, PHA/PA, PBS/PS, PLA/PET, PCL/PVC, PVA
3-microplastics	CCM (6) BBM (6)	PP, PA, PVC/PE, PS, PET/PP, PS, PVC/PE, PA, PET/PP, PA, PET/PE, PS, PVC PLA, PBS, PBAT/PCL, PVA, PHA/PLA, PVA, PBAT/PCL, PBS, PHA/PLA, PCL, PHA/PVA, PBS, PBAT
4-microplastics	CBM (9)	PP, PA, PLA, PCL/PE, PS, PBS, PBAT/PET, PVC, PA, PVA/PP, PS, PVA, PBAT/PE, PET, PLA, PHA/PA, PVC, PBS, PCL/PP, PVC, PLA, PBS/PE, PA, PHA, PBAT/PS, PET, PCL, PVA
6-microplastics	CBM (6)	PP, PA, PVC, PLA, PBS, PBAT/PE, PS, PET, PCL, PVA, PBAT/PP, PA, PET, PLA, PVA, PHA/PE, PS, PVC, PCL, PBS, PHA/PP, PS, PVC, PLA, PCL, PHA/PE, PA, PET, PVA, PBS, PBAT

<sup>a</sup>We setup the microplastic diversity gradients based on a random design (see [Materials and Methods](#) Section), and each sample was replicated for 4 times at two temperatures of 15 and 20 °C (CMps: PP = polypropylene, PE = high-density polyethylene, PET = poly(ethylene terephthalate), PS = polystyrene, PA = polyamide, PVC = poly(vinyl chloride); BMps: PLA = polylactic acid, PHA = polyhydroxyalkanoates, PVA = poly(vinyl alcohol), PBAT = poly(butylene adipate-co-terephthalate), PBS = polybutylene succinate, PCL = polycaprolactone, respectively). The groups of CCM and BBM represent the mixing of CMPs and BMPs only, and CBM represents mixing of CMPs and BMPs with a consistent ratio of 1:1, respectively. The numbers of compositions in each group are shown.

bial interaction affected by various microplastics in the real world presents a challenge, especially considering the additional influences of various global change factors, such as climate warming.<sup>20–22</sup>

Here, we examined the effects of microplastic diversity on bacterial ecological networks by developing novel microcosm experiments ([Figure 1b](#)). Specifically, we added in each microcosm 3 g of dried sediments, 9 mL of sterile water, 1 mL of microorganism solution, and 0.12 g of microplastic mixtures. The sediments were obtained from the Taihu Lake, the third largest lake in China, with a mean annual temperature

of 16.2 °C and microplastic abundance varying from 460 to 1,380 items/kg.<sup>23</sup> We selected 12 types of microplastics that are widely found in global lakes, which included 6 conventional microplastics (CMPs) and 6 biodegradable microplastics (BMPs).<sup>24</sup> To establish microplastic diversity, we considered three possible mixing strategies as observed in nature, that is, the mixing of only CMPs or BMPs (CCM or BBM) and another comixing of the CMPs and BMPs (CBM, where the weight ratio of CMPs and BMPs was 1:1), and obtained a microplastic richness gradient of 1, 2, 3, 4, and 6 using a random partition design<sup>25</sup> ([Table 1](#)). The random partition

design (also called the broken stick method) could maximize the separation of richness and compositional effects due to its nested approach.<sup>25–30</sup> We totally had 600 microcosms with or without microplastics and incubated them at 15 or 20 °C for 45 days. After collecting the microcosms, we examined the structure and composition of bacterial communities in the sediments and constructed SparCC co-occurrence networks at both temperatures (Figure 1b). We aimed to answer four main questions as follows: (1) Do microplastic mixing and temperature changes affect the microbial network structure such as complexity and stability? (2) Are there quantitative relationships between microplastic diversity and network complexity as well as stability in different temperatures? (3) Will the biodegradability of microplastics affect the microbial network characteries? (4) Whether there are interactive impacts of microplastic diversity, warming, and microplastic biodegradability on the network structures?

## MATERIALS AND METHODS

**Experimental Design and Microplastic Selection.** We setup 600 microcosms to obtain microplastic gradients from 1 to 6 types for incubation. In each microcosm, we used 20 mL headspace bottles and added 3 g of dried and homogenized sediments, 9 mL of sterilized pure water, 1 mL of bacterial solution, and 0.12 g of microplastic communities. We reserved a volume of 10 mL above the interior of each bottle and injected around 30 mL of high-purity nitrogen into the bottle to expel the original gas and equilibrated pressure. This allowed our systems to be rendered almost completely anaerobic and approximated natural deep lake sediment conditions. All microcosms were performed in the dark to avoid uncertainty due to the potential aging of microplastics by ultraviolet (UV) light.<sup>31</sup>

For each microcosm, we used the consistent and sterilized sediment sampling from the Taihu Lake (31.3357 N; 120.0808 E), China, in August 2018. Taihu Lake, the third largest freshwater lake in China, is a typical eutrophic lake with a booming economy and a large population of 36 million. Being strongly affected by human activities, the sediments of Taihu Lake were heavily contaminated with microplastics (460–1380 items/kg), and most of the local microplastic types (such as polypropylene, poly(ethylene terephthalate), and polylactic acid) could be found around the world lakes according to the previous study.<sup>23</sup> We next sieved and homogenized the sediments by grinding them to remove large debris, such as potential stones and observed plastics. The sediments were then sterilized at 121 °C for 30 min, dried at 110 °C for 24 h, and then aseptically dispensed into each vial for storage before incubating. In the week before the microcosm experiments in August 2022, we obtained sediments at the center of the Taihu Lake and stored them at 4 °C for 2 days to prepare for the bacterial solutions. We used a consistent and homogenized method to avoid other uncertainties in the experimental incubation process. Specifically, the bacterial solutions were obtained by serially diluting (1:10) a fresh sediment suspension sampled in sterile water using a 0.4 mm filter membrane (MF-Millipore), and the same bacterial solution of 1 mL was applied for each microcosm.<sup>32,33</sup> Finally, microcosms were preincubated in incubators at 15 or 20 °C for 45 days. As the local mean annual temperature was 16.2 °C, we designated the incubating microcosms at 20 °C as the warming group, while others were controls.

For microplastic diversity, we had a gradient from 1 to 6 types, which contains mixtures of conventional and/or biodegradable microplastics. We considered three microplastic mixing strategies that occur in natural environments, including the mixing of only CMPs (CCM) or BMPs (BBM) as well as another group containing both CMPs and BMPs with a consistent mixing ratio of 1:1 (CBM group), respectively. To construct microplastic diversity in the CCM and BBM groups, a random sampling without replacement was performed from the 6 types of CMPs or BMPs at microplastic richness of 2 or 3 with replicating 3 times, which allows all microplastics to occur in a given diversity gradient. For instance, the richness of 2 in the CCM or BBM group contains  $6/2 = 3$  microplastic compositions per sampling. The final CCM and BBM groups contained microplastic richness of 1, 2, and 3. For the CBM group, it was further nested from the combination of the same richness levels of the CCM and BBM groups, which resulted in 3 richness levels ( $R = 2, 4, \text{ and } 6$ ). Notably, the total weights of microplastics in each sample were constant, with 0.12 g, and each microcosm was even weighed. We replicated each sample 4 times and treated them with two constant temperatures of 15 and 20 °C.

All microplastics were purchased from Nraybiotech Co., Ltd. (Hunan province, China); they were milled and sieved to obtain particles of a defined size range, 50–300  $\mu\text{m}$ . In order to take into account the widespread microplastic pollution in lake sediments, we selected 6 types of CMPs, including polypropylene (PP), high-density polyethylene (HDPE, here remains named PE), poly(ethylene terephthalate) (PET), poly(vinyl chloride) (PVC), polystyrene (PS), and polyamide (PA). Similarly, for BMPs, we chose polylactic acid (PLA), polycaprolactone (PCL), poly(vinyl alcohol) (PVA), polyhydroxyalkanoates (PHA), polybutylene succinate (PBS), and poly(butylene adipate-co-terephthalate) (PBAT). Notably, we considered P<sub>3,4</sub>HB resin as the representative of PHA, which is a new commercial member of the PHA family, synthesized by microorganisms from renewable sources.<sup>34</sup> All 12 types of microplastics are found in lakes and watersheds around the world, especially traditional microplastics such as PP, PET, PS, and PHA.<sup>4,23,24</sup> The microplastics were thoroughly rinsed 5 times with deionized water and sterilized under 254 nm UV light for 10 min, then dried at 40 °C in an oven for 24 h, and finally stored in glass bottles separately before incubation experiments. Notably, the short-time UV lighting treatment would less likely cause the significant aging of the microplastics.<sup>35,36</sup>

**Microbial Community Characterization.** After 45 days of incubation, for each sample, microbial community DNA was extracted from 1.2 g of sediments after freezing–grinding, followed by purification using a MoBio PowerSoil DNA Isolation Kit (MoBio, Carlsbad). The 16S rRNA ribosome genes of bacteria and archaea were amplified using universal primers with 12bp barcode [Arch519F, 5'-CAGCCGCCGCGGTAA-3' and Arch915R, 5'-GTGCTCCCCGCCAATTCCT-3'] targeting the V4–5 version.<sup>37,38</sup> Primers were synthesized by Invitrogen (Carlsbad, CA). PCR reactions, containing 25  $\mu\text{L}$  of 2 $\times$  PremixTaq (Takara Biotechnology, Dalian Co. Ltd., China), 1  $\mu\text{L}$  of each primer (10 mM), and 3  $\mu\text{L}$  of DNA (20 ng/ $\mu\text{L}$ ) template in a volume of 50  $\mu\text{L}$ , were amplified by thermocycling: 5 min at 94 °C for initialization; 30 cycles of 30 s denaturation at 94 °C, 30 s annealing at 52 °C, and 30 s extension at 72 °C, followed by 10 min final elongation at 72 °C. We obtained amplification

products and normalized them at equal molar concentration and then paired-end sequenced ( $2 \times 250$ ) on the Illumina NovoSeq 6000/Miseq sequencing platform. Sequence reads were first filtered and potential primers were removed from the obtained 16S rRNA using DADA2 in QIIME2 V2022.8.3.<sup>39</sup> The above sequence processing was performed in QIIME2 V2022.8,<sup>40</sup> and then the filtered reads were deduplicated and denoised. After the paired-end sequences were merged and chimeras were removed, reads were truncated at a quality control score of 25. The taxonomic classification of each ASV of bacteria was obtained by aligning them against the SILVA 138 and UNITE databases by the *q2-feature-classifier* (sequence identity = 100%, using USEARCH *closed\_ref* command), respectively.<sup>41</sup> The fragments that could not be mapped were defined as unknown sequences. ASV tables were then generated based on the mapped sequences. The mapped ASV results for each dataset in USEARCH tabular format were imported directly into R software (version 3.6.0, R Core Team, 2019) and merged into the integrated ASV tables for further analysis. ASVs assigned to “mitochondria,” “chloroplasts,” “archaea,” and “eukaryotes” were removed from the bacterial communities. For each sample, the sequences of bacteria were consistently rarefied to 20,000.

**Network Construction and Structure Characterization.** To understand how microbial community networks vary along the microplastic richness gradient, we constructed SparCC networks using the “sparcc” function in R package SpiecEasi V1.1.2.<sup>42,43</sup> The SparCC is an algorithm that considers sparse component data in network construction and is more combinatorial robust than the traditional correlation analysis.<sup>42,44,45</sup> Specifically, a total of 18 networks (2 temperatures  $\times$  3 microplastic richness  $\times$  3 microplastic mixing strategies) were constructed, which allowed us to compare differences in network structure across groups. To ensure the reliability of the correlation calculations, species that occurred in at least 20% of the samples were selected.<sup>46</sup> We used 100 permutations to calculate the significance of correlations between taxon abundances and retained correlation matrices with correlations  $>0.4$  and significance  $<0.05$  for subsequent network construction. The degree distributions of all networks constructed in this study obeyed a power law of  $P(k) \sim k^{-\gamma}$  with significant  $R^2$  values (0.809–0.985, Table S2). According to the classification criteria, all networks are weakly scale-free.<sup>47</sup> The SparCC network graphs were plotted using R package igraph V1.4.0.<sup>48</sup>

We included various network topological parameters to represent the complexity and stability of species interactions among microbes. First, 9 metrics were calculated to characterize the topology of subnetworks using R package igraph, including the number of network nodes, links, connectance, average cluster coefficient, average degree, average path length, global efficiency, diameter, and average degree centrality.<sup>49,50</sup> These network complexity properties such as average degree and average degree centrality would help in understanding the complexity of biogeochemical transformations or the overall stability of ecosystems.<sup>51,52</sup> More detailed descriptions about these network properties are given in Table S1.

Second, we calculated the parameters to determine the network architecture, including network modularity and nestedness. Briefly, modularity measures the extent to which the network is divided into different modules, and links within those modules are distributed within rather than between distinct sets of nodes<sup>53</sup>; modules were compartmentalized

using the R function “cluster\_fast\_greedy” derived from R package igraph. Network nestedness measures the degree to which interactions can be arranged into subsets of the larger communities and ranges from 0 to 1, where 0 indicates that the network is not nested and 1 indicates that the network is fully nested.<sup>54</sup>

The significance of each parameter was assessed by comparing values of empirical networks to null models ( $N = 1000$ ) constructed with the method of *Swap.Web*.<sup>55</sup> Specifically, the means and standard deviations of the different topological parameters of these 1000 random networks were calculated and compared with the corresponding empirical networks. Metrics used to compare the empirical networks with the random networks are shown as  $Z$ -score values.<sup>55</sup> Compared to the random networks, empirical networks generally showed shorter average path length and higher connectivity (Table S2), which indicated that the constructed empirical networks exhibit small-world properties.<sup>56</sup>

Third, the classification of each node’s topological role in the network is made based on its intramodule connections ( $Z_i$ ) and intermodule connections ( $P_i$ ).<sup>57,58</sup> The keystone species, that is, identified module hubs ( $Z_i \geq 2.5$ ,  $P_i < 0.62$ ), connectors ( $Z_i < 2.5$ ,  $P_i \geq 0.62$ ), and network hubs ( $Z_i \geq 2.5$ ,  $P_i > 0.62$ ), were used for the common criterion in previous studies,<sup>53,59</sup> while all other nodes were categorized as peripherals. We calculated the numbers and relative proportions of keystone species within different empirical networks and observed their association with microplastic diversity.

Further, to validate the results of previous network complexity analysis, we selected the taxa presented in the 18 networks and calculated an abundance-weighted, zero-model-corrected metric based on the correlation of taxa in different samples, called Cohesion<sup>60</sup>

$$\text{cohesion} = \sum_{i=1}^m \text{abundance}_i \times \text{connectedness}_i \quad (1)$$

where  $m$  is the total number of taxa in a community. We used the “taxon shuffle” null model and the provided R code to calculate the positive and negative cohesion of each microbial community over time.<sup>60</sup> Two cohesion values (positive and negative) were calculated for each sample as the sum of significant positive or negative correlations between taxa weighted by the taxon abundance according to the above formula. Negative and positive cohesions range from  $-1$  to  $0$  and from  $0$  to  $1$ , respectively, with higher absolute values indicating greater or stronger correlations. We also calculated the ratio of negative to positive co-occurrence as the absolute value of negative:positive cohesion to determine whether richness better characterizes the processes driving negative correlations.<sup>61</sup> The relationships between network complexity and cohesion were characterized by Pearson correlation, while significant  $P$ -values were tested by multiple correction using the method of false discovery rate (FDR) estimation.<sup>62</sup>

Furthermore, we used two robustness tests based on multiple extinction simulations to test the stability of networks with regard to the microplastic diversity.<sup>63,64</sup> Based on previous studies,<sup>65</sup> we tested the robustness of each subnetwork using two different methods, including randomly removing nodes or target removing the most important nodes based on their betweenness centrality. The effect of species removal on the remaining network species was

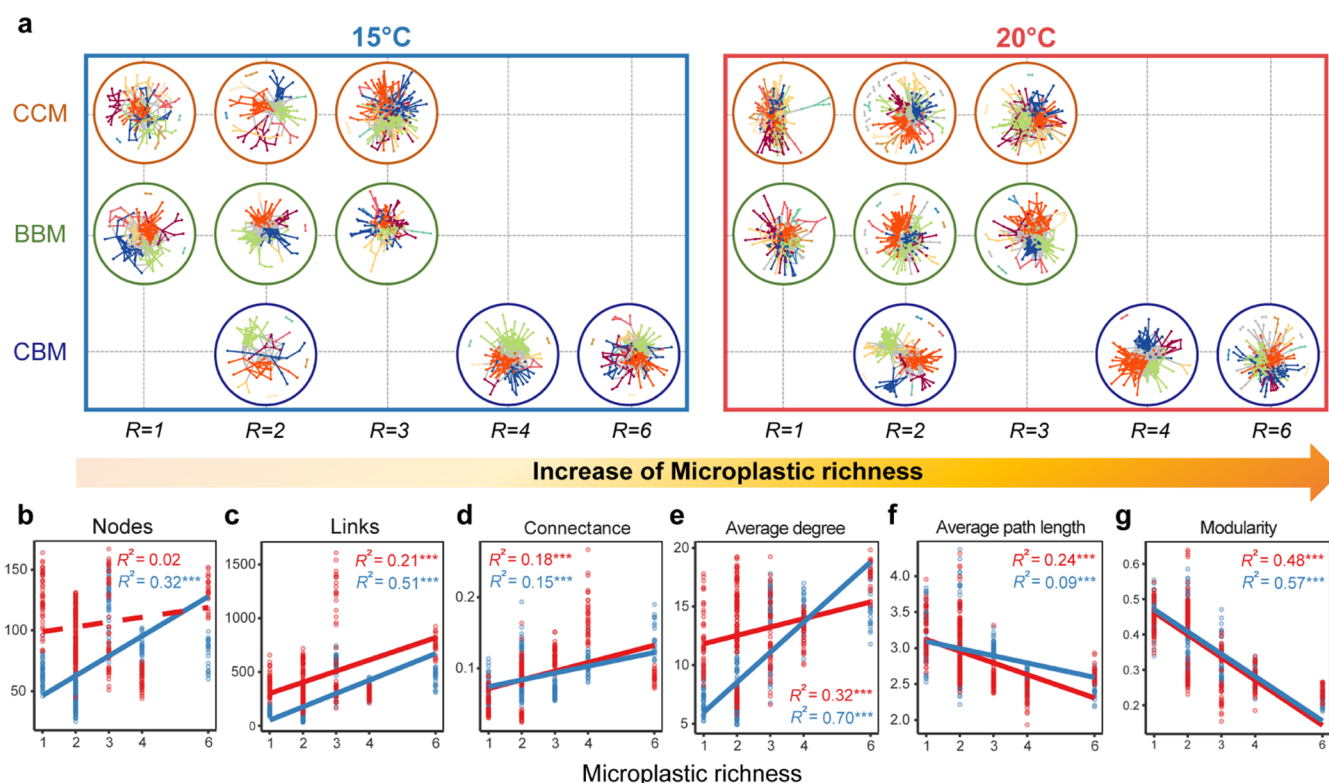


**Figure 2.** Links of microbial network topological parameters with microplastic diversity. (a) Visualization of the microbial networks for each microplastic diversity level. We showed correlations among the bacterial species according to each microplastic diversity level. The first 12 large modules with  $\geq 5$  nodes are shown in different colors, while smaller modules are shown in gray. In each panel, red borders indicate the microcosms that incubated at 20 °C, and blue borders indicate the incubation at 15 °C. The networks within orange, green, and blue circles represent three microplastic mixing strategies, that is, CCM, BBM, and CBM, respectively. Detailed information on empirical network topology attributes is listed in Table S2. (b–g) Relationships between network topological parameters and microplastic diversity based on the empirical networks partitioned into each sample subset, including the network number of nodes (b), number of links (c), connectance (d), average degree (e), average path length (f), and modularity (g). The relationships between microplastic diversity and network topology were tested using linear mixed-effects models, performed with the marginal  $R^2$  and significant  $P$ -values ( $*0.01 < P \leq 0.05$ ;  $**0.001 < P \leq 0.01$ ;  $***P \leq 0.001$ ). Detailed information on each model is listed in Table S4.

calculated from the abundance-weighted mean interaction strength (wMIS) of the remaining node  $i$

$$wMIS_i = \frac{\sum_{j \neq i} b_j S_{ij}}{\sum_{j \neq i} b_j} \quad (2)$$

where  $b_j$  is the relative abundance of species  $j$  and  $S_{ij}$  is the strength of the correlation with the SparCC method between species  $i$  and  $j$ . Thus, when random nodes are removed from the network, if  $wMIS_i \leq 0$ , node  $i$  is considered extinct/isolated (no species associated with node  $i$  exists or the remaining species is not sufficiently related), and it will be removed from the network. Therefore, after all extinct/isolated species have been removed (remaining  $wMIS_i > 0$ ), the proportion of remaining nodes in the network is defined as the network robustness. For each subnetwork, we simulated the effect of removing a 50% proportion of nodes at random 1000 times, and we calculated their mean robustness. In addition, we calculated the absolute values of the slope by fitting linear relationships between the proportion of randomly removed nodes and the proportion of remaining nodes in different subnetworks to characterize the network resistance under continuous external perturbations. The R codes for robustness tests were revised from those provided in the R package “ggClusterNet” V0.1.0<sup>66</sup> and at <https://github.com/Mengting-Maggie-Yuan/warming-network-complexity-stability>.<sup>65</sup>

In addition, we calculated the relationship between subnetwork vulnerability and microplastic diversity to further confirm the results of network stability. Vulnerability of a given node can characterize the relative contribution of that node to the global efficiency, while the global efficiency is calculated as the average of the efficiencies of all node pairs<sup>49,65</sup>

$$E = \frac{1}{n(n-1)} \sum_{i \neq j} \frac{1}{d(i,j)} \quad (3)$$

where  $d(i,j)$  is the number of edges on the shortest path between nodes  $i$  and  $j$ . Generally, the network vulnerability can be characterized as the maximum vulnerability of the node

$$\text{vulnerability} = \max\left(\frac{E - E_i}{E}\right) \quad (4)$$

where  $E$  is the global efficiency and  $E_i$  is the global efficiency after removing node  $i$  and all its links. The relationships between network complexity and stability were characterized by Pearson correlation, while the significance of  $P$ -value was tested by multiple correction using the method of “FDR.”

**Statistical Analysis.** To explore the effects of microplastic mixing on the bacterial network complexity and stability, we performed the linear mixed-effects models for various network parameters within both two temperatures as  $y \sim \text{Mixture} + (1\text{M})$  or  $y \sim \text{Mixture} + (1\text{M}) + (1\text{Bio})$  using R package lme4

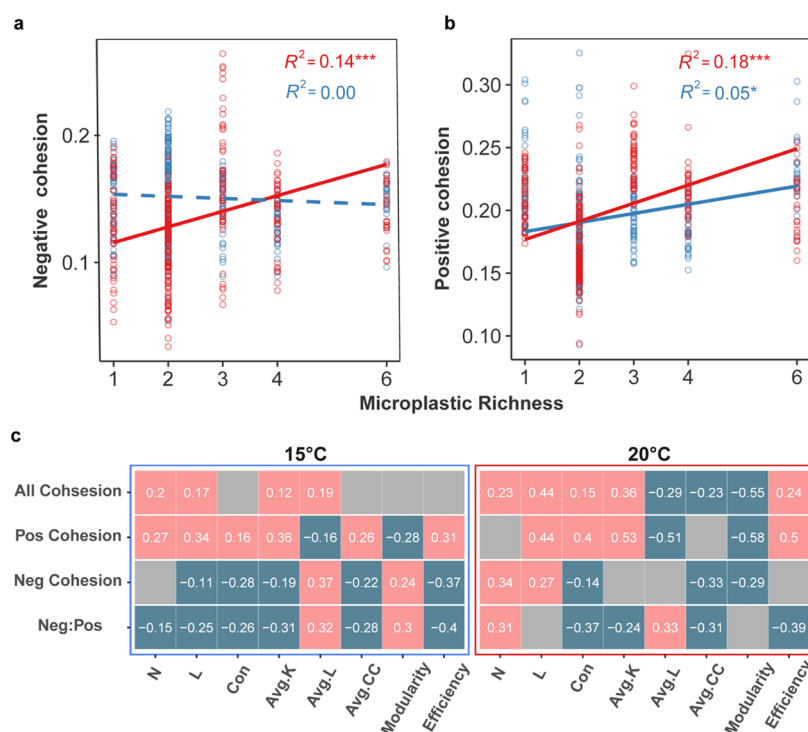


**Figure 3.** Links of cohesion of networked bacterial communities with microplastic diversity and network complexity indices. Relationships between positive cohesion (a) and negative cohesion (b) were shown using linear mixed-effects models, performed with marginal  $R^2$  and significant  $P$ -values ( $*0.01 < P \leq 0.05$ ;  $**0.001 < P \leq 0.01$ ;  $***P \leq 0.001$ ). In panels (a, b), red circles indicate the microcosms that incubated at 20 °C and blue borders indicate those at 15 °C. Details of each mixed linear model are listed in Table S5. (c) Pearson correlations of cohesion with various network complexity parameters at 15 °C (blue boxes) or 20 °C (red boxes). The “pos” and “neg” represent the positive and negative cohesion, respectively. Cells highlighted in pink or dark green indicate significant positive correlations or negative correlations ( $P \leq 0.05$ , after multiple correction of “FDR”), while those highlighted in gray indicate no significant correlations, respectively. The numbers in the cells are the correlation coefficients. Details of the correlation calculations are listed in Table S6.

V1.1–30.<sup>67</sup> Application of the model depends on the observed values of their Akaike information criterion (AIC). Here, we choose the latter model as the final model, as it had lower AIC values and a higher marginal  $R$  square than the former one. Among the models, a fixed effect of “Mixture” represents whether the added microplastics are mixed (as numeric values: 0 for single type of microplastic and 1 for microplastic mixtures), and a random factor “M” represents the combination of different types of microplastics (as a character, such as A and AB for groups that contained PP or both PP and PE, respectively), or the “Mixing” represents the proportion of biodegradable microplastics (as numeric values: the microplastic mixing strategies of CCM, BBM, and CBM were assigned as 0, 1, and 0.5, respectively). Conditional  $R$  square and marginal  $R$  square were calculated using  $R$  function “rsquaredGLMM” in MuMIn V1.47.1,<sup>68</sup> and statistical significance is based on Wald type II  $\chi^2$  tests using  $R$  function “Anova” in car V3.1–0,<sup>69</sup> after multiple correction using the method of “FDR.” For the microplastic diversity effects at different temperatures, the same procedure was performed. We also considered full models for network complexity and stability parameters to include the effects of microplastic diversity, temperature warming, and microplastic biodegradability as  $y \sim \text{richness} \times \text{temperature} \times \text{biodegradability} + (1| M)$ . We also extracted the regression coefficients ( $\beta$ ) for each model as effect sizes for different treatments. All statistical analyses were performed by specific packages of statistical software R V4.2.1.<sup>70</sup>

## RESULTS AND DISCUSSION

We investigated the impacts of microplastic mixing on various topological parameters of microbial networks, such as total links and connectance, using regression coefficients ( $\beta$ ) derived from linear mixed-effects models (see Materials and Methods Section). Briefly, compared to random networks, the constructed networks exhibited small-world properties with significantly higher network connectance and lower average path lengths ( $P < 0.001$ , Table S2). Specifically, compared to single type of microplastics, microbial networks among microcosms of microplastic mixtures showed significantly higher values of the total number of network links, average degree (average links per node), connectance (proportion of observed links among all possible links), average clustering coefficient (degree of node clustering), and average degree centrality (degree measures averaged node importance) in subnetworks, which was further supported by decreasing average path length ( $P < 0.05$ ; Table S3). These changes in network parameters such as more links, greater connectivity, and shorter path lengths could contribute to the faster transmission of external perturbative effects among networked species and thus enhance the efficiency of the system.<sup>71</sup> Further, compared to microcosms at 15 °C, the effects of microplastic mixing on the network complexity were generally greater at 20 °C, such as network average degree ( $\beta = 2.001$  and 3.0390 at 15 and 20 °C, respectively,  $P < 0.05$ ) and average path length ( $\beta = -0.072$  and  $-0.382$  at 15 and 20 °C, respectively,  $P < 0.01$ ; Table S3). Taken together, these results suggest that microplastic mixtures could enhance the network

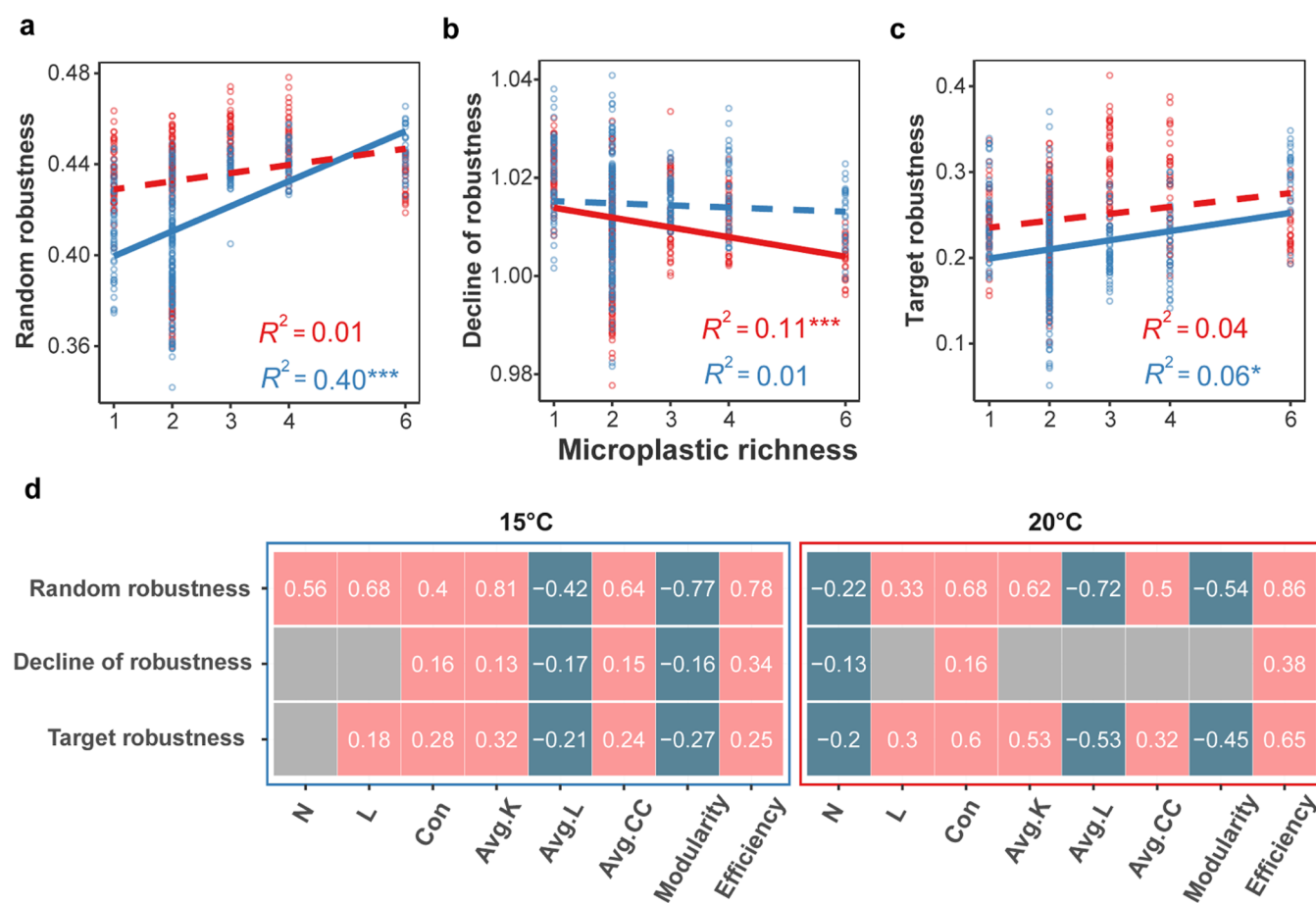


**Figure 4.** Microplastic diversity affects network stability and linking to the network structure. The robustness analysis showed the relationships between microplastic diversity and (a) the proportion of remaining nodes after randomly removing 50% of nodes, (b) the slope under continuous increase in the proportion of randomly removing nodes, and (c) robustness when removing 50% of the target nodes with maximum degree centrality. Blue lines indicate communities at 15 °C and red lines indicate communities at 20 °C, and the relationships were calculated using linear mixed-effects models, with marginal  $R^2$  and significant  $P$ -values being shown ( $*0.01 < P \leq 0.05$ ;  $**0.001 < P \leq 0.01$ ;  $***P \leq 0.001$ ). Details of each mixed linear model are listed in Table S8. (d) Pearson correlations of network stability with various network complexity parameters at 15 (blue boxes) and 20 °C (red boxes). Cells highlight in pink or dark green indicate significant positive correlations or negative correlations ( $P \leq 0.05$ , after multiple correction of “FDR”) and in gray indicate none significant correlations, respectively. The values shown in the cells are the coefficients of Pearson correlations. Details of the correlation calculations are listed in Table S9.

complexity, particularly under warmer temperatures. Notably, microbial networks estimated through co-occurrence-based analyses are more often recognized as hypothetical biological interactions and therefore need to be interpreted with great caution.<sup>72</sup>

Further quantitative evidence about the effects of microplastic mixing on network structures was supported by the positive correlation between network complexity and microplastic diversity, which was consistently observed under temperatures of 15 and 20 °C (Figures 2 and S1). Specifically, network connectance strongly increased along the microplastic diversity gradients at both temperatures ( $\beta = 0.010$  and  $0.014$  at 15 and 20 °C, respectively,  $P < 0.001$ ), which was also true for the average degree ( $\beta = 2.151$  and  $1.535$  at 15 and 20 °C, respectively,  $P < 0.001$ ), average degree centrality ( $\beta = 0.028$  and  $0.023$  at 15 and 20 °C, respectively,  $P < 0.001$ ), and global efficiency ( $\beta = 0.034$  and  $0.019$  at 15 and 20 °C, respectively,  $P < 0.05$ ), while the network average path length significantly decreased along the microplastic diversity ( $\beta = -0.098$  and  $-0.167$  at 15 and 20 °C, respectively,  $P < 0.001$ ; Figures 2, S1 and Table S4). Collectively, these findings imply that in response to increasingly complex microplastic contamination,

microbial communities could maintain more complex and efficient interactions.

Consistent with previous phenomenon, the degree of community connectivity among microbial networks was also strongly enhanced according to the microplastic diversity (Figures 3, S2, and Table S5). We used a metric of cohesion to quantify the strength of positive or negative associations between pairwise taxa to reveal the potential cooperative or competitive interactions, as well as the total species interaction indicated by sums of absolute positive and negative cohesion within a given sample.<sup>60</sup> Specifically, the total cohesion consistently increased with microplastic diversity in both temperatures ( $\beta = 0.005$  and  $0.027$  at 15 and 20 °C, respectively,  $P < 0.05$ ), which was true for positive cohesion ( $\beta = 0.006$  and  $0.014$  at 15 and 20 °C, respectively,  $P < 0.001$ ; Figures 3 and S2a). For negative cohesion, we only observed it strongly positively correlated to the microplastic diversity at higher temperatures ( $P < 0.001$ , Figure 3). Higher regression coefficients ( $\beta$ ) under warming also imply that increasing temperature amplified the effects of microplastic diversity on both positive and negative interactions within the microbial communities (Table S5). Moreover, we calculated the ratios of

Table 2. Treatment Effects on Microbial Network Complexity and Stability Based on Linear Mixed-Effects Models<sup>a</sup>

treatment		connectance	average degree	modularity	positive cohesion	negative cohesion	random robustness	target robustness
richness	$\beta$	<b>0.58</b>	<b>0.58</b>	<b>-0.62</b>	<b>0.24</b>	-0.27	<b>0.84</b>	<b>0.63</b>
	$\chi^2$	<b>76.98***</b>	<b>119.99***</b>	<b>154.52***</b>	<b>7.89**</b>	0.76	<b>33.95**</b>	<b>13.19**</b>
warming	$\beta$	0.06	<b>1.36</b>	<b>-0.51</b>	0.03	<b>-0.28</b>	<b>0.50</b>	<b>0.36</b>
	$\chi^2$	0.00	<b>676.46***</b>	<b>5.32*</b>	0.05	<b>90.04***</b>	<b>196.09***</b>	<b>64.42***</b>
biodegradability	$\beta$	<b>0.77</b>	<b>0.61</b>	<b>-1.16</b>	<b>0.59</b>	<b>-0.77</b>	<b>0.57</b>	<b>-0.10</b>
	$\chi^2$	<b>34.45***</b>	<b>9.60**</b>	<b>39.47***</b>	<b>13.23***</b>	<b>37.36***</b>	<b>34.35***</b>	<b>5.78*</b>
$R \times W$	$\beta$	<b>0.31</b>	<b>0.94</b>	-0.73	0.26	<b>0.61</b>	<b>0.38</b>	-0.16
	$\chi^2$	<b>14.39***</b>	<b>20.71***</b>	1.49	4.73	<b>28.88***</b>	<b>4.06*</b>	0.76
$B \times R$	$\beta$	-0.35	<b>0.20</b>	<b>-0.21</b>	-0.20	0.33	-0.58	<b>-0.77</b>
	$\chi^2$	2.87	<b>11.86***</b>	<b>4.37*</b>	0.93	0.01	3.74	<b>6.12*</b>
$W \times B$	$\beta$	-0.13	-1.07	<b>0.89</b>	-0.02	-0.54	<b>0.32</b>	0.37
	$\chi^2$	0.10	3.43	<b>10.12**</b>	0.28	3.33	<b>6.01*</b>	2.59
$R \times W \times B$	$\beta$	-0.20	-2.17	<b>1.53</b>	-0.26	-0.60	0.03	0.19
	$\chi^2$	0.65	<b>210.65***</b>	<b>125.08***</b>	0.80	4.78	0.02	0.37

<sup>a</sup>For each parameter, we performed a linear mixed-effects model of  $y \sim \text{richness} \times \text{temp} \times \text{bio} + (1|M)$ , where fixed effects included temperature change (temp, as a factor, 15 and 20 °C), microplastic richness (richness, as numeric values, ranging from 1 to 6 types), and microplastic degradability (bio, as numeric values, where different mixing strategies of CCM, BBM, and CBM were assigned as 0, 0.5, and 1, respectively), and random effects included the composition of different microplastics (M, as a character, such as A and AB represented plastic of PP or both PP and PE, respectively). Notably, here, all of the network parameters were rescaled. Statistical significance was calculated based on Wald type II  $\chi^2$  tests ( $n = 600$ ), using multiple correction of “FDR,” and significant effects are given in bold (\* $P < 0.05$ , \*\* $P < 0.01$ , and \*\*\* $P < 0.001$ ). The chisq-values ( $\chi^2$ ) are shown in the table. Supporting information of other parameters is listed in Table S10.

negative to positive cohesion to determine whether microplastic diversity drives negative association within networked species, which may be due to limited resource competition and niche divergence.<sup>60,61</sup> We found that this ratio significantly decreased along the microplastic diversity at 15 °C ( $\beta = -0.045$ ,  $P < 0.05$ ; Figure S2b), while showing a nonsignificant trend under higher temperature. The significant correlations between the cohesion and various network complexity indices were observed at both temperatures (averaged Pearson  $r = 0.22$  and  $0.28$  at 15 and 20 °C, respectively; Figure 3c and Table S6), which suggests that microplastic diversity could increase the complexity of microbial communities and thus possible interactions of species.<sup>61</sup>

The complexity of microbial networks in response to microplastic diversity also influenced network architecture, such as modularity (Figure 2g). In general, the constructed networks were highly modular and not nested, as indicated by the comparison between empirical networks and random networks (see Materials and Methods Section). A significantly decreasing trend in network modularity with microplastic diversity was observed at both temperatures ( $\beta = -0.063$  at 15 and 20 °C,  $P < 0.001$ ; Figure 2g and Table S4). Links within modules are distributed within rather than between different groups of nodes, so these nodes within different modules may represent the closely associated microbes (e.g., groups of coexisting or coevolving microbes).<sup>21</sup>

Based on within-module connections ( $Z_i$ ) and among-module connections ( $P_i$ ),<sup>57</sup> we determined a total of 422 connectors (nodes that link different modules), 39 module hubs (nodes that are highly connected to other modules), and 19 network hubs (nodes that are both module hubs and connectors) for all of the 18 empirical networks (Figure S3 and Table S7). All of these keystones could be considered as nodes that play vital roles in shaping the network structures,<sup>58</sup> in which the top three families of them are *Rhodocyclaceae* (7.0%, 29 of 414 keystones), followed by *Geobacteraceae* (5.8%, 24 of 414 keystones) and *Comamonadaceae* (5.3%, 22 of 414 keystones, Figure S4). Indeed, some of the keystones could

be a few taxa with excellent biodegradation of various plastics such as poly(ethylene terephthalate),<sup>73</sup> polyethylene,<sup>74</sup> polystyrene,<sup>75</sup> and other pollutants.<sup>76</sup> We found that microplastic diversity did not significantly change the proportion of keystones at either temperature nor did the number of keystones ( $P > 0.05$ , Figure S3). Keystone species are important for the structure and function of microbial communities,<sup>58</sup> and there remains large potential to use correlation analysis to find key microbial alliances that are associated with the biodegradation of microplastics.<sup>77,78</sup>

In addition, we found that higher microplastic diversity and temperature also led to more stable microbial networks (Figure 4 and Table S8). Network stability implies the resistance of systems to external perturbations and may positively correlate to network complexity.<sup>51,65,79</sup> Here, two robustness tests were used to simulate scenarios of species extinction and determine the proportion of remaining species in the networks, that is, (1) random removal of networked species or (2) targeted removal of species with the highest betweenness centrality, since nodes with higher betweenness centrality generally show greater impacts on the “information flow” through the networks.<sup>52,80</sup> Both results demonstrate that network robustness increased toward high microplastic diversity, especially at 15 °C ( $P < 0.05$ , Figure 4a,c). We also found that the network resistance along the microplastic diversity gradients increased more significantly at 20 °C ( $P < 0.05$ , Figure 4b). These effects are further supported by the significantly negative correlations between network vulnerability and microplastic diversity at both temperatures (Table S4). Moreover, we found that increasing the temperature generally enhanced the microplastic diversity effects on microbial network stability as the networks were generally more robust and less vulnerable at higher temperatures (Tables 1 and S10). We also found that network stability and complexity parameters showed strong correlations, such as average degree, modularity, and global efficiency at both temperatures (averaged Pearson  $r = 0.34$  and  $0.37$  at 15 and 20 °C, respectively; Figure 4d and Table S9). Collectively, these results suggest that microbial networks were more robust

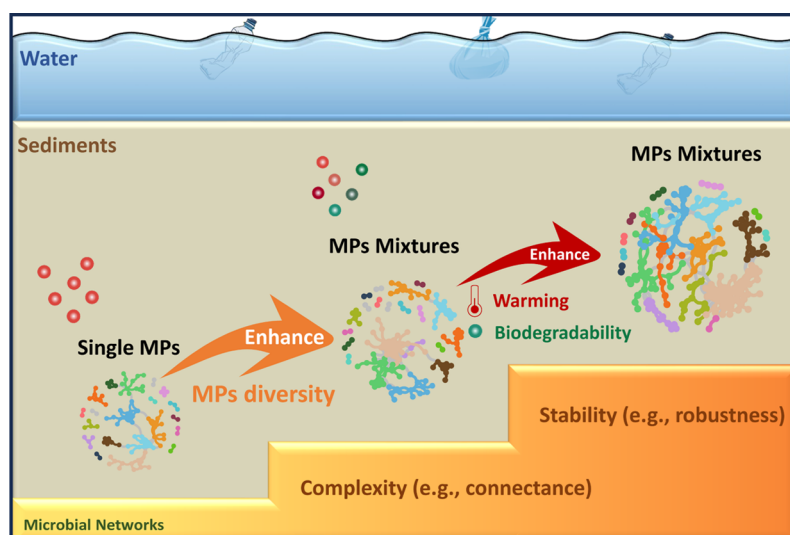


**Figure 5.** Influences of microplastic mixtures on microbial networks in lake sediments. Various types of plastics are degraded into small particles of microplastics that retained in lake sediment ecosystems and form the microplastic mixtures (MPs mixtures) and thus microplastic diversity (MPs diversity). Compared to single-type microplastics (Single MPs), microbial networks under the occurrence of microplastic mixtures are more complex and stable. This is because microplastic diversity significantly enhances the complexity (e.g., connectance and species interactions) and stability (e.g., robustness) of the networks. Climate warming and the presence of biodegradable microplastics could further increase the complexity and stability of the networks.

under higher microplastic diversity and temperature, which could be associated with their direct or potential interactive effects on the network complexity.

Finally, we incorporated microplastic diversity, temperature change, and microplastic biodegradability in the linear mixed-effects model to comprehensively investigate their direct and interactive effects on the network structure and stability. Generally, increasing microplastic diversity and warming showed the most significant direct effects on network topology parameters such as numbers of network nodes, total links, connectance, average degree, modularity, positive cohesion, and robustness ( $\chi^2 = 13.23$  to  $676.46$ ,  $P < 0.001$ ; Figure S5). Interestingly, microplastic diversity and increasing temperature further showed synergistic impacts for various network parameters. For instance, higher microplastic diversity and temperatures jointly enhanced most of the indices of network complexity in the same way ( $\chi^2 = 5.81$  to  $114.84$ ,  $P < 0.05$ ; Table 2). In addition, microplastic biodegradability (here represented by different microplastic mixing strategies) was another potential factor contributing to changes in the network complexity and stability (Figure S5). For instance, elevating the proportion of biodegradable microplastics generally enhanced the network complexity and stability, including the network connectance, global efficiency, positive cohesion and random robustness, and reduced average path length, positive cohesion, and modularity ( $\chi^2 = 13.23$  to  $83.01$ ,  $P < 0.05$ ; Tables 2 and S10). This is consistent with the analysis of the interactive and positive effects of microplastic diversity on network complexity. Compared to conventional microplastics, biodegradable microplastics may act as more bioavailable substrates (e.g., nonrecalcitrant carbon), thus could lead to an increase in microbial metabolic activity and potential interactions related to resource utilization and ecological niche differentiation.<sup>81,82</sup>

Assessing the biological consequences of complex and diverse microplastic pollution is one of the main objectives of recent ecological environmental governance.<sup>6,83</sup> However,

few studies quantitatively assess the effects of environmental microplastic mixtures on the community composition and biotic interactions of microbes. Our findings provide empirical evidence that microplastic diversity significantly and predictably enhanced the complexity and stability of microbial interactions in lake sediments (Figure 5). After 45 days of laboratory incubation, ecological networks of bacteria affected by microplastic mixtures strongly became more complex compared to single type of microplastics, especially at higher temperature. Increasing diversity from 1 to 6 types of microplastics predictably increased network complexity of bacteria at both temperatures, such as increasing network links, connectance, and average degree, as well as decreasing network average path length, which led the network to be more robust. Importantly, the microplastic diversity effects on the ecological network complexity and species interactions were further amplified under warming. In addition to the direct or interactive effects of microplastic diversity and warming, we also demonstrated that higher proportions of biodegradable microplastic strongly strengthened the network complexity and stability. By deploying novel experiments considering microplastic mixing and their diversity, our findings provide important implications for the ecological impacts of complex microplastic pollution. In addition to microplastic richness, more research needs to capture their other potential diversity index such as chemistry, aging, sizes, and shapes.<sup>84</sup> In the future, capturing temporal impacts of complex microplastics on microbial communities is also necessary, especially considering the emergence of biodegradable microplastics.<sup>13,14,85</sup> With increasing microplastic pollution and climate warming, environmental microbial communities will become more cohesive and robust regarding their species interactions; this may further influence related ecosystem functions.

## ■ ASSOCIATED CONTENT

### Data Availability Statement

The 16S sequence data generated in this study are available in the NODE (<https://www.biosino.org/node>): OEP004225. All data supporting the findings are available online in the Supporting Information.

### SI Supporting Information

The Supporting Information is available free of charge at <https://pubs.acs.org/doi/10.1021/acs.est.3c08704>.

Additional information on the description of network properties used in this study; characterization of empirical network topological parameters regarding microplastic diversity; microplastic mixing effects on network parameters; microplastic diversity effects on cohesion; Pearson correlation between network structures and cohesion; microplastic diversity effects on network robustness; Pearson correlation between parameters of network complexity and stability; treatment effects on microbial network parameters of complexity and stability; links of microplastic diversity with network parameters; links of microplastic diversity with cohesion; identification of network keystone species and their links to microplastic diversity; proportions of keystone species taxon family in different networks; treatment direct effects on network complexity and stability (PDF)

Summary of keystone species according to microplastic diversity (XLSX)

## ■ AUTHOR INFORMATION

### Corresponding Author

Jianjun Wang – State Key Laboratory of Lake Science and Environment, Nanjing Institute of Geography and Limnology, Chinese Academy of Sciences, Nanjing 210008, China; [orcid.org/0000-0001-7039-7136](https://orcid.org/0000-0001-7039-7136); Email: [jjwang@niglas.ac.cn](mailto:jjwang@niglas.ac.cn)

### Authors

Hao Wu – State Key Laboratory of Lake Science and Environment, Nanjing Institute of Geography and Limnology, Chinese Academy of Sciences, Nanjing 210008, China; College of Oceanography, Hohai University, Nanjing 210098, China; [orcid.org/0000-0001-5887-1106](https://orcid.org/0000-0001-5887-1106)

Tianheng Gao – State Key Laboratory of Lake Science and Environment, Nanjing Institute of Geography and Limnology, Chinese Academy of Sciences, Nanjing 210008, China; College of Marine Science and Engineering, Nanjing Normal University, Nanjing, Jiangsu 210023, China

Ang Hu – State Key Laboratory of Lake Science and Environment, Nanjing Institute of Geography and Limnology, Chinese Academy of Sciences, Nanjing 210008, China

Complete contact information is available at: <https://pubs.acs.org/10.1021/acs.est.3c08704>

### Author Contributions

<sup>||</sup>H.W. and T.G. contributed equally to this work. J.W. developed the original ideas presented in the manuscript. H.W. performed the laboratory experiments and statistical analyses with assistance of J.W., T.G., and A.H. H.W. wrote the first draft, and J.W., T.G., and A.H. jointly revised the

manuscript. All authors contributed to the intellectual development of this study.

### Notes

The authors declare no competing financial interest.

## ■ ACKNOWLEDGMENTS

We appreciate Xu Ma, Shuyu Jiang, Jianing Xu, Fanfan Meng, Yanan Zhou, Xiwen Xiao, Ming Chen, Wenlei Xue, and Yifan Wu for assistance of laboratory experiments. This study was supported by the National Natural Science Foundation of China (42225708, 92251304, and 42307112).

## ■ REFERENCES

- (1) Rochman, C. M. Microplastics research—from sink to source. *Science* **2018**, *360* (6384), 28–29.
- (2) Rochman, C. M.; Hoellein, T. The global odyssey of plastic pollution. *Science* **2020**, *368* (6496), 1184–1185.
- (3) Multiple ocean threats *Nat. Ecol. Evol.* **2023**; Vol. 7783 DOI: [10.1038/s41559-023-02099-5](https://doi.org/10.1038/s41559-023-02099-5).
- (4) Nava, V.; Chandra, S.; Aherne, J.; Alfonso, M. B.; Antão-Geraldes, A. M.; Attermeyer, K.; Bao, R.; Bartrons, M.; Berger, S. A.; Biernaczyk, M.; Bissen, R.; Brookes, J. D.; Brown, D.; Cañedo-Argüelles, M.; Canle, M.; Capelli, C.; Carballeira, R.; Cereijo, J. L.; Chawchai, S.; Christensen, S. T.; Christoffersen, K. S.; de Eyto, E.; Delgado, J.; Dornan, T. N.; Doubek, J. P.; Dusaucy, J.; Erina, O.; Ersoy, Z.; Feuchtmayr, H.; Frezzotti, M. L.; Galafassi, S.; Gateuille, D.; Gonçalves, V.; Grossart, H.-P.; Hamilton, D. P.; Harris, T. D.; Kangur, K.; Kankılıç, G. B.; Kessler, R.; Kiel, C.; Krynak, E. M.; Leiva-Presa, A.; Lepori, F.; Matias, M. G.; Matsuzaki, S.-i. S.; McElarney, Y.; Messyasz, B.; Mitchell, M.; Mlambo, M. C.; Motitsoe, S. N.; Nandini, S.; Orlandi, V.; Owens, C.; Özkundakci, D.; Pinnow, S.; Pociecha, A.; Raposeiro, P. M.; Rööm, E.-I.; Rotta, F.; Salmaso, N.; Sarma, S. S. S.; Sartirana, D.; Scordo, F.; Sibomana, C.; Siewert, D.; Stepanowska, K.; Tavşanoğlu, Ü. N.; Tereshina, M.; Thompson, J.; Tolotti, M.; Valois, A.; Verburg, P.; Welsh, B.; Wesolek, B.; Weyhenmeyer, G. A.; Wu, N.; Zawisza, E.; Zink, L.; Leoni, B. Plastic debris in lakes and reservoirs. *Nature* **2023**, *619* (7969), 317–322.
- (5) Corinaldesi, C.; Canensi, S.; Dell'Anno, A.; Tangherlini, M.; Di Capua, I.; Varrella, S.; Willis, T. J.; Cerrano, C.; Danovaro, R. Multiple impacts of microplastics can threaten marine habitat-forming species. *Commun. Biol.* **2021**, *4* (1), No. 431.
- (6) Revell, L. E.; Kuma, P.; Le Ru, E. C.; Somerville, W. R. C.; Gaw, S. Direct radiative effects of airborne microplastics. *Nature* **2021**, *598* (7881), 462–467.
- (7) MacLeod, M.; Arp, H. P. H.; Tekman, M. B.; Jahnke, A. The global threat from plastic pollution. *Science* **2021**, *373* (6550), 61–65.
- (8) Parashar, N.; Hait, S. Plastic rain—Atmospheric microplastics deposition in urban and peri-urban areas of Patna City, Bihar, India: Distribution, characteristics, transport, and source analysis. *J. Hazard. Mater.* **2023**, *458*, No. 131883.
- (9) Rillig, M. C.; Leifheit, E.; Lehmann, J. Microplastic effects on carbon cycling processes in soils. *PLOS Biol.* **2021**, *19* (3), No. e3001130.
- (10) Worm, B.; Lotze, H. K.; Jubinville, I.; Wilcox, C.; Jambeck, J. Plastic as a Persistent Marine Pollutant. *Annu. Rev. Environ. Resour.* **2017**, *42* (1), 1–26.
- (11) Reid, A. J.; Carlson, A. K.; Creed, I. F.; Eliason, E. J.; Gell, P. A.; Johnson, P. T. J.; Kidd, K. A.; MacCormack, T. J.; Olden, J. D.; Ormerod, S. J.; Smol, J. P.; Taylor, W. W.; Tockner, K.; Vermaire, J. C.; Dudgeon, D.; Cooke, S. J. Emerging threats and persistent conservation challenges for freshwater biodiversity. *Biol. Rev.* **2019**, *94* (3), 849–873.
- (12) de Souza Machado, A. A.; Kloas, W.; Zarfl, C.; Hempel, S.; Rillig, M. C. Microplastics as an emerging threat to terrestrial ecosystems. *Global Change Biol.* **2018**, *24* (4), 1405–1416.
- (13) Su, X.; Yang, L.; Yang, K.; Tang, Y.; Wen, T.; Wang, Y.; Rillig, M. C.; Rohe, L.; Pan, J.; Li, H.; Zhu, Y.-g. Estuarine plastisphere as an

- overlooked source of N<sub>2</sub>O production. *Nat. Commun.* **2022**, *13* (1), No. 3884.
- (14) Amaral-Zettler, L. A.; Zettler, E. R.; Mincer, T. J. Ecology of the plastisphere. *Nat. Rev. Microbiol.* **2020**, *18* (3), 139–151.
- (15) Sheridan, E. A.; Fonvielle, J. A.; Cottingham, S.; Zhang, Y.; Dittmar, T.; Aldridge, D. C.; Tanentzap, A. J. Plastic pollution fosters more microbial growth in lakes than natural organic matter. *Nat. Commun.* **2022**, *13* (1), No. 4175.
- (16) Shi, J.; Sun, Y.; Wang, X.; Wang, J. Microplastics reduce soil microbial network complexity and ecological deterministic selection. *Environ. Microbiol.* **2022**, *24* (4), 2157–2169.
- (17) Rong, L.; Zhao, L.; Zhao, L.; Cheng, Z.; Yao, Y.; Yuan, C.; Wang, L.; Sun, H. LDPE microplastics affect soil microbial communities and nitrogen cycling. *Sci. Total Environ.* **2021**, *773*, No. 145640.
- (18) Li, K.; Jia, W.; Xu, L.; Zhang, M.; Huang, Y. The plastisphere of biodegradable and conventional microplastics from residues exhibit distinct microbial structure, network and function in plastic-mulching farmland. *J. Hazard. Mater.* **2023**, *442*, No. 130011.
- (19) Sun, Y.; Li, X.; Cao, N.; Duan, C.; Ding, C.; Huang, Y.; Wang, J. Biodegradable microplastics enhance soil microbial network complexity and ecological stochasticity. *J. Hazard. Mater.* **2022**, *439*, No. 129610.
- (20) Hu, A.; Choi, M.; Tanentzap, A. J.; Liu, J.; Jang, K.-S.; Lennon, J. T.; Liu, Y.; Soininen, J.; Lu, X.; Zhang, Y.; Shen, J.; Wang, J. Ecological networks of dissolved organic matter and microorganisms under global change. *Nat. Commun.* **2022**, *13* (1), No. 3600.
- (21) Yang, G.; Ryo, M.; Roy, J.; Lammel, D. R.; Ballhausen, M.-B.; Jing, X.; Zhu, X.; Rillig, M. C. Multiple anthropogenic pressures eliminate the effects of soil microbial diversity on ecosystem functions in experimental microcosms. *Nat. Commun.* **2022**, *13* (1), No. 4260.
- (22) Sun, S.; Hu, X.; Kang, W.; Yao, M. Combined effects of microplastics and warming enhance algal carbon and nitrogen storage. *Water Res.* **2023**, *233*, No. 119815.
- (23) Zhang, Q.; Liu, T.; Liu, L.; Fan, Y.; Rao, W.; Zheng, J.; Qian, X. Distribution and sedimentation of microplastics in Taihu Lake. *Sci. Total Environ.* **2021**, *795*, No. 148745.
- (24) Dusaucy, J.; Gateuille, D.; Perrette, Y.; Naffrechoux, E. Microplastic pollution of worldwide lakes. *Environ. Pollut.* **2021**, *284*, No. 117075.
- (25) Bell, T.; Lilley, A. K.; Hector, A.; Schmid, B.; King, L.; Newman, J. A. A Linear Model Method for Biodiversity–Ecosystem Functioning Experiments. *Am. Nat.* **2009**, *174* (6), 836–849.
- (26) Mallon, C. A.; Poly, F.; Le Roux, X.; Marring, I.; van Elsas, J. D.; Salles, J. F. Resource pulses can alleviate the biodiversity–invasion relationship in soil microbial communities. *Ecology* **2015**, *96* (4), 915–926.
- (27) Rivett, D. W.; Scheuerl, T.; Culbert, C. T.; Mombrikotb, S. B.; Johnstone, E.; Barraclough, T. G.; Bell, T. Resource-dependent attenuation of species interactions during bacterial succession. *ISME J.* **2016**, *10* (9), 2259–2268.
- (28) Gravel, D.; Bell, T.; Barbera, C.; Bouvier, T.; Pommier, T.; Venail, P.; Mouquet, N. Experimental niche evolution alters the strength of the diversity–productivity relationship. *Nature* **2011**, *469* (7328), 89–92.
- (29) Bruelheide, H.; Nadrowski, K.; Assmann, T.; Bauhus, J.; Both, S.; Buscot, F.; Chen, X.-Y.; Ding, B.; Durka, W.; Erfmeier, A.; Gutknecht, J. L. M.; Guo, D.; Guo, L.-D.; Härdtle, W.; He, J.-S.; Klein, A.-M.; Kühn, P.; Liang, Y.; Liu, X.; Michalski, S.; Niklaus, P. A.; Pei, K.; Scherer-Lorenzen, M.; Scholten, T.; Schuldt, A.; Seidler, G.; Trogisch, S.; von Oheimb, G.; Welk, E.; Wirth, C.; Wubet, T.; Yang, X.; Yu, M.; Zhang, S.; Zhou, H.; Fischer, M.; Ma, K.; Schmid, B. Designing forest biodiversity experiments: general considerations illustrated by a new large experiment in subtropical China. *Methods Ecol. Evol.* **2014**, *5* (1), 74–89.
- (30) Bestion, E.; Haegeman, B.; Alvarez Codesal, S.; Garreau, A.; Huet, M.; Barton, S.; Montoya, J. M. Phytoplankton biodiversity is more important for ecosystem functioning in highly variable thermal environments. *Proc. Natl. Acad. Sci. U.S.A.* **2021**, *118* (35), No. e2019591118.
- (31) Mao, R.; Lang, M.; Yu, X.; Wu, R.; Yang, X.; Guo, X. Aging mechanism of microplastics with UV irradiation and its effects on the adsorption of heavy metals. *J. Hazard. Mater.* **2020**, *393*, No. 122515.
- (32) van Elsas, J. D.; Chiurazzi, M.; Mallon, C. A.; Elhottová, D.; Kristůfek, V.; Salles, J. F. Microbial diversity determines the invasion of soil by a bacterial pathogen. *Proc. Natl. Acad. Sci. U.S.A.* **2012**, *109* (4), 1159–1164.
- (33) Hu, A.; Jang, K.-S.; Tanentzap, A. J.; Zhao, W.; Lennon, J. T.; Liu, J.; Li, M.; Stegen, J.; Choi, M.; Lu, Y.; Feng, X.; Wang, J. Thermal responses of dissolved organic matter under global change. *Nature Communications* **2024**, *15*, 576.
- (34) Luo, R.; Xu, K.; Chen, G.-Q. Study of miscibility, crystallization, mechanical properties, and thermal stability of blends of poly(3-hydroxybutyrate) and poly(3-hydroxybutyrate-co-4-hydroxybutyrate). *J. Appl. Polym. Sci.* **2007**, *105* (6), 3402–3408.
- (35) Song, Y. K.; Hong, S. H.; Jang, M.; Han, G. M.; Jung, S. W.; Shim, W. J. Combined Effects of UV Exposure Duration and Mechanical Abrasion on Microplastic Fragmentation by Polymer Type. *Environ. Sci. Technol.* **2017**, *51* (8), 4368–4376.
- (36) Liu, H.; Zhang, X.; Ji, B.; Qiang, Z.; Karanfil, T.; Liu, C. UV aging of microplastic polymers promotes their chemical transformation and byproduct formation upon chlorination. *Sci. Total Environ.* **2023**, *858*, No. 159842.
- (37) Yang, Y.; Dai, Y.; Wu, Z.; Xie, S.; Liu, Y. Temporal and Spatial Dynamics of Archaeal Communities in Two Freshwater Lakes at Different Trophic Status. *Front. Microbiol.* **2016**, *7*, No. 451.
- (38) Zhang, X.; Li, Y.; Lei, J.; Li, Z.; Tan, Q.; Xie, L.; Xiao, Y.; Liu, T.; Chen, X.; Wen, Y.; Xiang, W.; Kuzjakov, Y.; Yan, W. Time-dependent effects of microplastics on soil bacteriome. *J. Hazard. Mater.* **2023**, *447*, No. 130762.
- (39) Callahan, B. J.; McMurdie, P. J.; Rosen, M. J.; Han, A. W.; Johnson, A. J. A.; Holmes, S. P. DADA2: High-resolution sample inference from Illumina amplicon data. *Nat. Methods* **2016**, *13* (7), 581–583.
- (40) Bolyen, E.; Rideout, J. R.; Dillon, M. R.; Bokulich, N. A.; Abnet, C. C.; Al-Ghalith, G. A.; Alexander, H.; Alm, E. J.; Arumugam, M.; Asnicar, F.; et al. Reproducible, interactive, scalable and extensible microbiome data science using QIIME 2. *Nat. Biotechnol.* **2019**, *37* (8), 852–857.
- (41) Gurevich, A.; Saveliev, V.; Vyahhi, N.; Tesler, G. QIIME 2: quality assessment tool for genome assemblies. *Bioinformatics* **2013**, *29* (8), 1072–1075.
- (42) Kurtz, Z. D.; Müller, C. L.; Miraldi, E. R.; Littman, D. R.; Blaser, M. J.; Bonneau, R. A. Sparse and compositionally robust inference of microbial ecological networks. *PLoS Comput. Biol.* **2015**, *11* (5), No. e1004226.
- (43) Kurtz, Z.; Mueller, C.; Miraldi, E.; Bonneau, R. SpiecEasi: Sparse inverse covariance for ecological statistical inference *R Package Version 2017*.
- (44) Friedman, J.; Alm, E. J. Inferring correlation networks from genomic survey data. *PLoS Comput. Biol.* **2012**, *8* (9), No. e1002687.
- (45) Weiss, S.; Van Treuren, W.; Lozupone, C.; Faust, K.; Friedman, J.; Deng, Y.; Xia, L. C.; Xu, Z. Z.; Ursell, L.; Alm, E. J.; Birmingham, A.; Cram, J. A.; Fuhrman, J. A.; Raes, J.; Sun, F.; Zhou, J.; Knight, R. Correlation detection strategies in microbial data sets vary widely in sensitivity and precision. *ISME J.* **2016**, *10* (7), 1669–1681.
- (46) Faust, K. Open challenges for microbial network construction and analysis. *ISME J.* **2021**, *15* (11), 3111–3118.
- (47) Broido, A. D.; Clauset, A. Scale-free networks are rare. *Nat. Commun.* **2019**, *10* (1), No. 1017.
- (48) Csardi, G.; Nepusz, T. The igraph software package for complex network research. *InterJournal, Complex Syst.* **2006**, *1695* (5), 1–9.
- (49) Deng, Y.; Jiang, Y.-H.; Yang, Y.; He, Z.; Luo, F.; Zhou, J. Molecular ecological network analyses. *BMC Bioinform.* **2012**, *13*, No. 113.

- (50) Lau, M. K.; Borrett, S. R.; Baiser, B.; Gotelli, N. J.; Ellison, A. M. Ecological network metrics: opportunities for synthesis. *Ecosphere* **2017**, *8* (8), No. e01900.
- (51) Hillebrand, H.; Langenheder, S.; Leuret, K.; Lindström, E.; Östman, Ö.; Striebel, M. Decomposing multiple dimensions of stability in global change experiments. *Ecol. Lett.* **2018**, *21* (1), 21–30.
- (52) Bissett, A.; Brown, M. V.; Siciliano, S. D.; Thrall, P. H. Microbial community responses to anthropogenically induced environmental change: towards a systems approach. *Ecol. Lett.* **2013**, *16* (s1), 128–139.
- (53) Olesen, J. M.; Bascompte, J.; Dupont, Y. L.; Jordano, P. The modularity of pollination networks. *Proc. Natl. Acad. Sci. U.S.A.* **2007**, *104* (50), 19891–19896.
- (54) Almeida-Neto, M.; Guimarães, P.; Guimarães, P. R., Jr.; Loyola, R. D.; Ulrich, W. A consistent metric for nestedness analysis in ecological systems: reconciling concept and measurement. *Oikos* **2008**, *117* (8), 1227–1239.
- (55) Dormann, C. F.; Fründ, J.; Blüthgen, N.; Gruber, B. Indices, graphs and null models: analyzing bipartite ecological networks. *Open Ecol. J.* **2009**, *2*, 7–24.
- (56) Watts, D. J.; Strogatz, S. H. Collective dynamics of ‘small-world’ networks. *Nature* **1998**, *393* (6684), 440–442.
- (57) Röttgers, L.; Faust, K. Can we predict keystones? *Nat. Rev. Microbiol.* **2019**, *17* (3), 193.
- (58) Banerjee, S.; Schlaeppli, K.; van der Heijden, M. G. A. Keystone taxa as drivers of microbiome structure and functioning. *Nat. Rev. Microbiol.* **2018**, *16* (9), 567–576.
- (59) Shi, S.; Nuccio, E. E.; Shi, Z. J.; He, Z.; Zhou, J.; Firestone, M. K. The interconnected rhizosphere: High network complexity dominates rhizosphere assemblages. *Ecol. Lett.* **2016**, *19* (8), 926–936.
- (60) Herren, C. M.; McMahon, K. D. Cohesion: a method for quantifying the connectivity of microbial communities. *ISME J.* **2017**, *11* (11), 2426–2438.
- (61) Hernandez, D. J.; David, A. S.; Menges, E. S.; Searcy, C. A.; Afkhami, M. E. Environmental stress destabilizes microbial networks. *ISME J.* **2021**, *15* (6), 1722–1734.
- (62) Noble, W. S. How does multiple testing correction work? *Nat. Biotechnol.* **2009**, *27* (12), 1135–1137.
- (63) Montesinos-Navarro, A.; Hiraldo, F.; Tella, J. L.; Blanco, G. Network structure embracing mutualism–antagonism continuums increases community robustness. *Nat. Ecol. Evol.* **2017**, *1* (11), 1661–1669.
- (64) Dunne, J. A.; Williams, R. J.; Martinez, N. D. Food-web structure and network theory: the role of connectance and size. *Proc. Natl. Acad. Sci. U.S.A.* **2002**, *99* (20), 12917–12922.
- (65) Yuan, M. M.; Guo, X.; Wu, L.; Zhang, Y.; Xiao, N.; Ning, D.; Shi, Z.; Zhou, X.; Wu, L.; Yang, Y.; Tiedje, J. M.; Zhou, J. Climate warming enhances microbial network complexity and stability. *Nat. Clim. Change* **2021**, *11* (4), 343–348.
- (66) Wen, T.; Xie, P.; Yang, S.; Niu, G.; Liu, X.; Ding, Z.; Xue, C.; Liu, Y.-X.; Shen, Q.; Yuan, J. ggClusterNet: An R package for microbiome network analysis and modularity-based multiple network layouts. *iMeta* **2022**, *1* (3), No. e32.
- (67) Bates, D.; Mächler, M.; Bolker, B.; Walker, S. Fitting Linear Mixed-Effects Models Using lme4. *J. Stat. Software* **2015**, *67* (1), 1–48.
- (68) Anderson, D.; Burnham, K. *Model Selection and Multi-Model Inference*; Springer, 2004; Vol. 63.
- (69) Fox, J.; Weisberg, S. *An R Companion to Applied Regression*; Sage Publications, 2018.
- (70) Team, R. C.. R: A Language and Environment for Statistical Computing; R Foundation for Statistical Computing: Vienna, Austria. <http://www.R-project.org/>.
- (71) Montoya, J. M.; Pimm, S. L.; Solé, R. V. Ecological networks and their fragility. *Nature* **2006**, *442* (7100), 259–264.
- (72) Blanchet, F. G.; Cazelles, K.; Gravel, D. Co-occurrence is not evidence of ecological interactions. *Ecol. Lett.* **2020**, *23* (7), 1050–1063.
- (73) Yoshida, S.; Hiraga, K.; Takehana, T.; Taniguchi, I.; Yamaji, H.; Maeda, Y.; Toyohara, K.; Miyamoto, K.; Kimura, Y.; Oda, K. A bacterium that degrades and assimilates poly(ethylene terephthalate). *Science* **2016**, *351* (6278), 1196–1199.
- (74) Taipale, S. J.; Peltomaa, E.; Kukkonen, J. V. K.; Kainz, M. J.; Kautonen, P.; Tirola, M. Tracing the fate of microplastic carbon in the aquatic food web by compound-specific isotope analysis. *Sci. Rep.* **2019**, *9* (1), No. 19894.
- (75) Liu, R.; Zhao, S.; Zhang, B.; Li, G.; Fu, X.; Yan, P.; Shao, Z. Biodegradation of polystyrene (PS) by marine bacteria in mangrove ecosystem. *J. Hazard. Mater.* **2023**, *442*, No. 130056.
- (76) Yadav, R.; Rajput, V.; Dharme, M. Functional metagenomic landscape of polluted river reveals potential genes involved in degradation of xenobiotic pollutants. *Environ. Res.* **2021**, *192*, No. 110332.
- (77) Yu, Y.; Miao, L.; Adyel, T. M.; Waldschläger, K.; Wu, J.; Hou, J. Aquatic plastisphere: Interactions between plastics and biofilms. *Environ. Pollut.* **2023**, *322*, No. 121196.
- (78) Han, Y.; Teng, Y.; Wang, X.; Ren, W.; Wang, X.; Luo, Y.; Zhang, H.; Christie, P. Soil Type Driven Change in Microbial Community Affects Poly(butylene adipate-co-terephthalate) Degradation Potential. *Environ. Sci. Technol.* **2021**, *55* (8), 4648–4657.
- (79) Thébaud, E.; Fontaine, C. Stability of Ecological Communities and the Architecture of Mutualistic and Trophic Networks. *Science* **2010**, *329* (5993), 853–856.
- (80) Barberán, A.; Bates, S. T.; Casamayor, E. O.; Fierer, N. Using network analysis to explore co-occurrence patterns in soil microbial communities. *ISME J.* **2012**, *6* (2), 343–351.
- (81) Dey, S.; Rout, A. K.; Behera, B. K.; Ghosh, K. Plastisphere community assemblage of aquatic environment: plastic-microbe interaction, role in degradation and characterization technologies. *Environ. Microbiome* **2022**, *17*, No. 32.
- (82) Yang, Y.; Liu, W.; Zhang, Z.; Grossart, H.-P.; Gadd, G. M. Microplastics provide new microbial niches in aquatic environments. *Appl. Microbiol. Biotechnol.* **2020**, *104* (15), 6501–6511.
- (83) Bank, M. S.; Mitrano, D. M.; Rillig, M. C.; Lin, C. S. K.; Ok, Y. S. Embrace complexity to understand microplastic pollution. *Nat. Rev. Earth Environ.* **2022**, *3* (11), 736–737.
- (84) Rillig, M. C.; Leifheit, E.; Lehmann, J. Microplastic effects on carbon cycling processes in soils. *PLOS Biol.* **2021**, *19* (3), No. e3001130.
- (85) Rillig, M. C.; Kim, S. W.; Zhu, Y.-G. The soil plastisphere. *Nat. Rev. Microbiol.* **2023**, *22*, 64–74.